Journal of Non-Crystalline Solids xxx (2012) xxx–xxx

Contents lists available at SciVerse ScienceDirect

Journal of Non-Crystalline Solids

journal homepage: www.elsevier.com/ locate/ jnoncrysol

Density of states evaluations from oscillating/moving grating techniques

F. Ventosinos [a,*], C. Longeaud [b], J.A. Schmidt [a]

[a] INTEC (UNL-CONICET), Güemes 3450, 3000 Santa Fe, Argentina, and FIQ (UNL), Santiago del Estero 2829, 3000 Santa Fe, Argentina
[b] Laboratoire de Génie Electrique de Paris, (UMR 8507 CNRS) Ecole Supérieure d'Electricité, Universités Paris VI et XI, Plateau de Moulon, 91192 Gif-sur-Yvette CEDEX, France

ARTICLE INFO

Article history:
Received 2 August 2011
Received in revised form 23 November 2011
Available online xxxx

Keywords:
Semiconductors;
Photoconductivity;
Amorphous silicon;
Grating techniques

ABSTRACT

In this paper we first present a comparison between two grating techniques, the oscillating photocarrier grating (OPG) and the moving grating technique (MGT). The common origin of both techniques suggests that they should give the same experimental data. In this work we present measurements performed with both techniques and show their equivalence. Regarding the fact that the OPG method uses a lock-in amplifier to measure the photocurrent, while the MGT uses an electrometer due to its dc nature, we show that these techniques can be used in a complementary way, using the benefits that each one of them offers. Moreover, we present measurements of the density of states (DOS) of an amorphous silicon sample, which were made using a range of temperatures that are only achievable using both techniques. We also present a brief summary of the theory supporting these techniques, and we outline future research to improve the DOS estimation.

© 2011 Elsevier B.V. All rights reserved.

1. Introduction

Photocarrier grating techniques are based on making interference between two coherent light beams to form a periodic pattern of light intensity on a sample surface. Areas of high and low light intensities result in high and low carrier concentrations, respectively, which create an internal electric field. In the past decades these kinds of techniques were used to estimate the diffusion length of minority carriers in materials with photovoltaic applications [1], to study their electrical transport properties [2] and to test the assumption of ambipolar transport [3].

It is also well known that the density of states (DOS) in the gap of amorphous semiconductors is of great interest because the localized states govern the transport properties of these materials. Moreover, procedures to extract part of the DOS from measurements involving grating techniques have been proposed [4,5]. Very recently, the oscillating photocarrier grating (OPG) technique emerged as a promising technique to estimate the DOS of hydrogenated amorphous silicon (a-Si:H) [6]. In that publication, the authors argue that the OPG can be considered an ac version of the moving grating technique (MGT) proposed some time ago by Haken et al. [2]. One of the purposes of this work is to verify experimentally the equivalence between the OPG and MGT techniques. We will also show that these techniques are complementary, allowing us to measure quantities over a wide range of conditions that are very difficult to achieve with only one of these techniques. Finally, we will implement experimentally the DOS spectroscopy that was outlined in Ref. [6].

The paper is organized as follows: In Section 2 we will explain briefly both techniques and their experimental setup. In Section 3 a short summary of the basic equations needed to understand the underlying physics is given. Section 4 shows the experimental comparison to test the equivalence between these two techniques. In Section 5 we will outline a DOS spectroscopy and show the experimental results. Finally, Section 6 presents the main conclusions of this work.

2. Experimental setup

The experimental setup used for both techniques is shown in Fig. 1. The light source is a He–Ne laser because its red light, although having an energy larger than the bandgap of a-Si:H, is uniformly absorbed. The laser light, linearly polarized in the vertical direction, is split into two coherent beams that finally interfere on the position of the sample. One of the beams (attenuated to an intensity I_2) impinges perpendicular to the sample, while the other one (of intensity I_1) forms an angle δ with the other beam. Therefore, an intensity grating with spatial period $\Lambda = \frac{\lambda}{\sin(\delta)}$ is created, where λ is the light wavelength. In the MGT technique, two acousto-optic modulators are used to introduce a small frequency shift Δf between the beams, which causes the intensity grating to move with a constant velocity proportional to Δf. The resulting illumination intensity is found to be $I = I_0 + \delta I \cos[k(x - v_{gr}t)]$, where $I_0 = I_1 + I_2$, $\delta I = 2\sqrt{I_1 I_2}$, $v_{gr} = \Lambda\Delta f$,

* Corresponding author.
E-mail addresses: fventosinos@intec.unl.edu.ar, fedevento@gmail.com (F. Ventosinos).

0022-3093/$ – see front matter © 2011 Elsevier B.V. All rights reserved.
doi:10.1016/j.jnoncrysol.2011.12.046

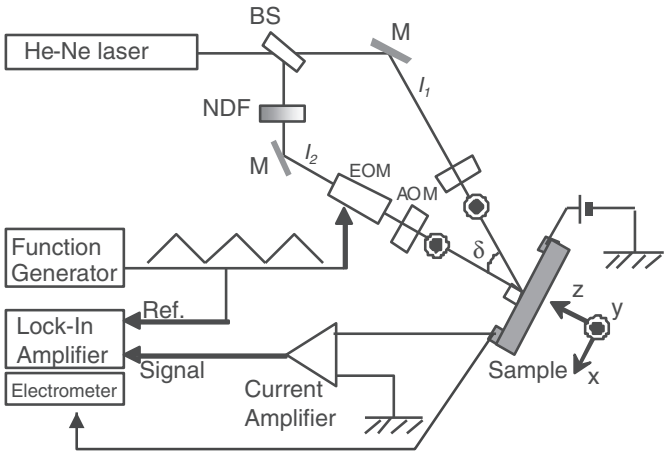

Fig. 1. Experimental setup for the experiment. A linearly polarized laser beam is split by a beam splitter (BS) into two beams, I_1 and I_2, which are made to coincide on the sample by using the mirrors (M). Beam I_2, attenuated by a neutral density filter (NDF), passes through an electro-optic modulator (EOM) used as a phase modulator (OPG) or through acousto-optic modulators (MGT) to obtain a small shift in their frequencies. The lock-in amplifier measures the ac photocurrent due to the oscillating grating, whereas the electrometer is used to read the dc current generated in MGT configuration.

and $k=\frac{2\pi}{\Lambda}$ [2]. The experimental quantity that is measured with an electrometer is a dc short circuit current, resulting from the movement of the intensity grating.

In the OPG technique, the two acousto-optic modulators are replaced by a single electro-optic modulator (EOM) used to control the phase of beam I_2, while beam I_1 remains unaltered. In order to have control of the phase of beam I_2, the EOM is positioned with the axes of the crystal vertical and horizontal. In this 'phase modulation' configuration, the output amplitude and polarization remain unchanged, but the phase of the wave (ϕ) can be varied as a function of the signal applied to the modulator. When this function is a triangular wave function, the calculation of the resulting illumination intensity impinging the sample gives $I=I_0+\delta I\cos(kx\pm\omega t)$, where ω is the angular frequency of the triangular wave and the other symbols have the same meaning as before. The result is an intensity grating that moves with a constant velocity in one direction for the first half of each period (therefore for half a grating period) and then moves in the opposite direction for the second half of each period. In this way we can think of OPG as an ac version of MGT, allowing us to use synchronous detection with a lock-in amplifier, and therefore improving the signal to noise ratio.

3. Basic equations

The transport equations for electrons and holes are:

$$\frac{\partial n(x,t)}{\partial t}=G(x,t)-R_n(x,t)+\mu_n\frac{\partial}{\partial x}[n(x,t)\xi(x,t)]+D_n\frac{\partial^2 n(x,t)}{\partial x^2},$$

$$\frac{\partial p(x,t)}{\partial t}=G(x,t)-R_p(x,t)-\mu_p\frac{\partial}{\partial x}[p(x,t)\xi(x,t)]+D_p\frac{\partial^2 p(x,t)}{\partial x^2}.$$

Here, $n(x,t)$ and $p(x,t)$ are the free electrons and holes concentrations, $G(x,t)$ is the generation rate, $R_{n,p}(x,t)$ is the electron (hole) recombination rate, $\mu_{n,p}$ is the electron (hole) mobility, and $D_{n,p}$ is the electron (hole) diffusion constant. $\xi(x,t)$ is the total electric field, composed by an (optional) external electric field and an internal electric field related to the electrons and holes concentrations via Poisson's equation

$$\frac{d\xi_{\text{int}}(x)}{dx}=\frac{q}{\varepsilon\varepsilon_0}\left\{p(x)+\int_{E_v}^{E_c}[1-f(E,x,t)]N^{DON}(E)dE-n(x)-\int_{E_v}^{E_c}f(E,x,t)N^{ACC}(E)dE\right\}$$

where ε is the dielectric constant of the sample, ε_0 is the dielectric permittivity of vacuum, E_v is the energy at the top of the valence band, E_c is the energy at the bottom of the conduction band, $f(E,x,t)$ is the occupation function, $N^{DON}(E)$ is the density of donor states (neutral when occupied and positively charged when unoccupied), and $N^{ACC}(E)$ is the density of acceptor states (neutral when empty and negatively charged when occupied). The recombination terms are:

$$R_n(x,t)=\int_{E_v}^{E_c}\{c_n n(x,t)[1-f(E,x,t)]-e_n(E)f(E,x,t)\}N(E)dE,$$

$$R_p(x,t)=\int_{E_v}^{E_c}\left\{c_p p(x,t)f(E,x,t)-e_p(E)[1-f(E,x,t)]\right\}N(E)dE,$$

where c is the capture coefficient, $e(E)$ is the emission rate and $N(E)$ is the DOS. The expression for the generation rate depends on the technique that we consider. As can be seen in Ref. [6], for OPG the generation rate can we written as $G_{\pm}(x,t)_{OPG}=G_0+\delta G\cos(kx\pm\omega t)=G_0+\Re e\left[\delta G e^{i(kx\pm\omega t)}\right]$, where G_0 and δG relate to the homogeneous and modulated parts of the illumination I_0 and δI, respectively, $i^2=-1$, and $\Re e$ means the real part of the complex number. For MGT [2] the term becomes $G(x,t)_{MGT}=G_0+\delta G\cos\left(k\left(x-v_{gr}t\right)\right)=G_0+\Re e\left[\delta G e^{i\left(k\left(x-v_{gr}t\right)\right)}\right]$.

To solve the transport equations we will assume low-modulation condition (i.e., $I_1\gg I_2$, granted by the use of a neutral density filter). This means that it is expected that the relevant physical parameters vary sinusoidally as $G(x,t)$ does. In general, however, there will be variable phase shifts, and any quantity A can be expressed as $A(x,t)=A_0+\Re e\left[\ \delta A\ \ e^{i(kx+\omega t)}\right]$, where A_0 is the value under uniform illumination G_0, and δA is a complex magnitude originating from the modulated term of the generation rate δG. Introducing these expressions for $n(x,t)$, $p(x,t)$ and $\xi(x,t)$ into the differential transport equations, together with Poisson's equation, linearizes the system. The solutions for $n(x,t)$ and $p(x,t)$ are complicated functions of the DOS involving integrals over the gap. To handle these solutions we developed a computer code, which calculates the generated photocurrent as

$$j(t)=\frac{1}{\Lambda}\int_0^{\Lambda}\left[q\mu_n n(x,t)+q\mu_p p(x,t)\right][\xi_{ext}+\xi_{\text{int}}(x,t)]dx=j_0+\Delta j(t).$$

In Ref. [6] we made a complete analysis of the physics involved in the OPG experiment, explaining the origin of the photocurrent, its dependence on the frequency ω and the typical shape of the OPG/MGT curves.

4. Results

4.1. Comparison between both techniques

When solving the transport equations for electrons and holes, it is clear that the only difference between both methods is the expression of the generation rate. But if we analyze carefully these terms we will see, as already explained, that both techniques have a common origin, which is a grating moving with constant velocity. In OPG this happens for the first half of the period; then the grating travels in the opposite direction—but with the same grating speed. Therefore, by using both

Please cite this article as: F. Ventosinos, et al., Density of states evaluations from oscillating/moving grating techniques, J. Non-Cryst. Solids (2012), doi:10.1016/j.jnoncrysol.2011.12.046

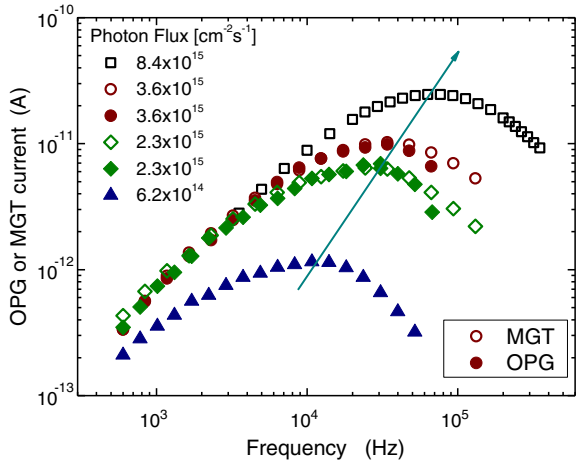

Fig. 2. Measurements of OPG (solid symbols) and MGT (open symbols) techniques, performed for four different photon fluxes. For MGT the frequency is $\Delta f = {}^{v_{gr}}/_{\Lambda}$. As can be seen, there is a range of fluxes where both techniques can be used, giving the same results. For lower generation rates the photoconductivity is too low to be measured by an electrometer. For higher values the OPG has bandwidth limitations.

techniques we should obtain the same current. In Fig. 2 we show measurements performed on the same a-Si:H sample using both techniques. Every point in the graph is the result of 60 measurements taken every 1 s. The error bars are smaller than the size of the points.

From Fig. 2 it is clear that, when the same photon flux is used, both techniques give the same curve ($\Phi = 2.3$ and $3.6\times10^{15}\,\mathrm{cm^{-2}\,s^{-1}}$). For lower values of the generation rate the photoconductivity is very small (of the order of a few pA), which are very difficult to read with an electrometer. Given the fact that OPG uses a current amplifier and a lock in amplifier, these small values of photocurrent can still be measured. Therefore, OPG is the most suitable technique when the level of the signal is low, as shown in Fig. 2 for $\Phi = 6.2\times10^{14}\,\mathrm{cm^{-2}\,s^{-1}}$.

As can be seen in Fig. 2, an increase in the photon flux causes the maximum of the curves to shift to higher angular frequencies. At high frequencies some problems with the bandwidths of the current amplifier and the lock-in amplifier start to appear, limiting the applicability of the OPG technique. On the other hand, the MGT does not suffer from these problems, because it gives a dc current. Moreover, the increase of the signal makes the dc current easier to measure, making the MGT the most suitable method for the higher photon fluxes, as shown in Fig. 2 for $\Phi = 8.4\times10^{15}\,\mathrm{cm^{-2}\,s^{-1}}$. We have also made measurements varying the temperature at which the experiment is performed, keeping constant the photon flux. The variation of the temperature causes a similar effect as the variation of the generation rate. For lower temperatures, OPG is best suited because of the small currents involved. There is a range of temperatures where both techniques can be used, and for higher temperatures MGT is more appropriate because it avoids the bandwidth limitations of OPG.

The combination of temperature and photon flux defines which technique is better to use, but as can be seen these techniques can be used in a complementary way, covering a wide range of temperature/photon flux conditions. This will be very useful in the next section, when trying to achieve a DOS spectroscopy by using the value of angular frequency that gives the maximum conductivity ($\omega_{\max}$).

5. Discussion

5.1. DOS spectroscopy from OPG/MGT measurements

In Ref. [6] we have demonstrated that $\omega_{\max}^{-1}$ is related to some characteristic time of the sample, which can be the dielectric relaxation time (τ_{diel}) or the small signal lifetime for electrons (τ_n'). We have also shown that the small signal lifetime is related to the density of states at the electrons quasi-Fermi level, E_{Fn}, by the approximate equation

$$N(E_{Fn}) \cong \frac{G_0 \tau_n'}{k_B T \gamma}. \tag{1}$$

Here, G_0 is the homogenous generation rate, T is the absolute temperature, k_B is Boltzman's constant and γ is the exponent of the proportionality relation between photoconductivity and generation rate, i.e., $\sigma_0 \propto G_0^{\gamma}$. Since the electron's quasi-Fermi level is sensitive to changes in temperature and/or photon flux, a DOS spectroscopy can be achieved by varying any of these parameters.

In Fig. 3 we show with solid symbols the DOS that results from applying Eq. (1) to the experimental curves (like those of Fig. 2). The measurements were made on a light-soaked a-Si:H sample to avoid changes in the DOS during the experiment. The temperature was varied between 133 and 413 K in steps of 20 K. OPG was used for the points at lower temperatures (133 to 203 K), while the rest of the data were measured with the MGT. The error bars displayed in Fig. 3, which have almost the same size of the points, are primarily due to the uncertainty in the estimation of $\omega_{\max}$. To estimate this error, we calculate the frequency difference between two consecutive points in the surroundings of $\omega_{\max}$. For temperatures higher than 423 K the contribution of the dark current to the photocurrent ceases to be negligible, putting an upper limit to the temperatures that can be used. In order to be in the lifetime regime, where we have $\omega_{\max}^{-1} \approx \tau_n'$, we have used high photon fluxes of $2.98\times10^{17}\,\mathrm{cm^{-2}\,s^{-1}}$ (triangles) and $1.49\times10^{17}\,\mathrm{cm^{-2}\,s^{-1}}$ (stars).

In Ref. [7] we have shown that the approximate Eq. (1) can be further refined, obtaining for the conduction band tail region

$$N^{CBT}(E_{Fn}) = \frac{G_0 \tau_n'}{k_B T \gamma F}, \tag{2}$$

where the correction factor is given by $F = \dfrac{(1-\alpha)\pi}{\sin(\alpha\pi)}$, with $\alpha = 1 + \dfrac{T}{T_C}$, being T_C the characteristic temperature of the conduction band tail. Application of Eq. (2) to the measured data leads to the DOS plotted with open circles in Fig. 3. Using this data we are able to estimate important parameters of the DOS in the upper half of the bandgap. For this sample the experimental results suggest an exponential conduction band tail with a slope of ~0.042 meV, and a distribution of deep states that can characterized by a Gaussian having a maximum value around $1.7\times10^{17}\,\mathrm{cm^{-3}\,eV^{-1}}$, a standard deviation of ~0.1 eV

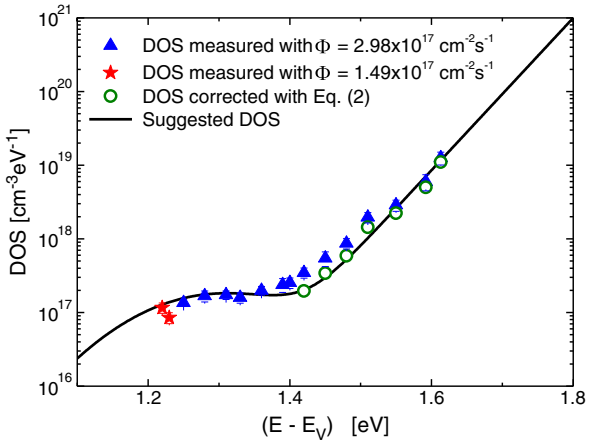

Fig. 3. Measured DOS (symbols) using OPG and MGT techniques. The triangles were measured with a photon flux of $2.98\times10^{17}\,\mathrm{cm^{-2}\,s^{-1}}$ while for the stars it was $1.5\times10^{17}\,\mathrm{cm^{-2}\,s^{-1}}$. The open circles are the measurements for the conduction band tail corrected by the application of Eq. (2), while the solid line is the DOS suggested by the measurements.

Please cite this article as: F. Ventosinos, et al., Density of states evaluations from oscillating/moving grating techniques, J. Non-Cryst. Solids (2012), doi:10.1016/j.jnoncrysol.2011.12.046

ARTICLE IN PRESS

and centered at ~1.30 eV. The slope of the conduction band tail may be considered rather high compared to previously reported values, which range between 25 and 34 meV [8]. However, we note that the sample used in these experiments was fully light-soaked, and as pointed out in Ref. [9] the conduction band tail may take higher values after light soaking, also increasing the characteristic slope. Regardless of these facts, we should point out that the technique that we propose to recover information on the DOS is in a preliminary stage and should be tested against other techniques to assess its power of resolution. In particular, modulated photoconductivity (MPC) measurements [10] will be performed to confirm and compare the DOSs obtained by both techniques.

To have access to other parameters, such as electron mobility or capture coefficients, the OPG-MGT measurements can be complemented with data from other techniques. The MPC technique, for example, gives a relative DOS that includes the ratio between the capture coefficient and the electron mobility [10]. Using both measurements we are confident to be able to estimate more parameters that are needed to characterize amorphous semiconductors materials.

6. Conclusions

The first aim of this work was to check that OPG and MGT techniques were able to be use together, so as to take advantage of the benefits that each one can offer. OPG technique can deal with noisy situations such as low photon fluxes or low temperatures, but it is bandwidth limited. On the other hand, while MGT fails to measure when the flux or the temperature is too low, it does not have any bandwidth limitation since it is a dc technique. The result of this comparison was satisfying, i.e., there is a range of photon fluxes in which both techniques give the same curve; for lower values OPG gives better results, and for higher values only MGT can be used.

The other aim of this work was to implement experimentally the DOS spectroscopy outlined in Ref. [6]. We made measurements using both techniques and we were able to obtain the DOS of the a-Si:H sample used for these experiments. We could characterize the conduction band tail and part of the deep states. To go further in the characterization of the material we will link these grating methods to other techniques such as the MPC.

Acknowledgments

This work was partly supported by MINCyT (Project 22-32515), CONICET (Project PIP 1464), UNL (Project CAI + D 68-349) and ECOS Sud-MINCyT (Project A08E01).

References

[1] D. Ritter, E. Zeldov, K. Weiser, Appl. Phys. Lett. 49 (1986) 791–793.
[2] U. Haken, M. Hundhausen, L. Ley, Phys. Rev. B. 51 (1995) 10579–10590.
[3] K. Hattori, Y. Koji, S. Fukuda, W. Ma, H. Okamoto, J. Appl. Phys. 73 (1993) 3846–3851.
[4] J.A. Schmidt, C. Longeaud, Phys. Rev. B. 71 (2005) 1252081–1252813.
[5] J.A. Schmidt, N. Budini, F. Ventosinos, C. Longeaud, Phys. Status Solidi A. 207 (2010) 556–560.
[6] F. Ventosinos, N. Budini, C. Longeaud, J.A. Schmidt, J. Phys. D: Appl. Phys. 44 (2011) 2951031–29510312.
[7] C. Longeaud and J. A. Schmidt, "*a-Si:H transport parameters from experiments based on photoconductivity*", Journal of Non-Crystalline Solids, this issue.
[8] D.V. Lang, J.D. Cohen, J.P. Harbison, Phys. Rev. B 25 (1982) 5285–5320.
[9] C. Longeaud, D. Roy, Z. Teukam Hangouan, Appl. Phys. Lett. 77 (2000) 3604–3606.
[10] C. Longeaud, J.P. Kleider, Phys. Rev. B. 45 (1992) 11672–11684.

Please cite this article as: F. Ventosinos, et al., Density of states evaluations from oscillating/moving grating techniques, J. Non-Cryst. Solids (2012), doi:10.1016/j.jnoncrysol.2011.12.046